A Model of Composite Solid-Propellant Combustion Based on Multiple Flames

M. W. Beckstead,* R. L. Derr,† and C. F. Price‡
Lockheed Propulsion Company, Redlands, Calif.

A model describing the combustion of AP composite propellants has been developed. The model is based on a flame structure surrounding individual oxidizer crystals; the relationship between crystals and the binder matrix being evaluated statistically. Three separate flame zones are considered: 1) a primary flame between the decomposition products of the binder and the oxidizer, 2) a premixed oxidizer flame, and 3) a final diffusion flame between the products of the other two flames. Simple global kinetics are assumed for gas-phase reactions, and the surface decomposition of the propellant ingredients is assumed to be adequately described by simple Arrhenius expressions. The oxidizer decomposition is taken as being the over-all controlling factor in the combustion process. The results obtained show that the calculated surface temperature and the effect of oxidizer concentration predicted by the model are in agreement with observed experimental trends. The predicted effect of particle size is somewhat greater than observed experimentally while the temperature sensitivity is in excellent agreement with experimental data. The results of the calculations indicate a relatively strong exothermic reaction taking place at the propellant surface. Apparently the ammonium perchlorate (AP) partially decomposes exothermically in the thin surface melt previously reported in AP deflagration studies.

Nomenclature

A = Arrhenius frequency factor
A_{fh} = ratio of the peak diffusional distance to the effective heat-transfer distance of the diffusion flame
b = burner radius from Burke-Schumann analysis; also the characteristic surface dimension [see Eq. (14)]
c_2 = constant in Eq. (13): $\mathfrak{D}_0 T^{1.75} W/R$
c_p = average mean heat capacity for the solid and gases
d = characteristic diffusion dimension [see Eq. (12)]
D_0 = diameter of oxidizer crystal before combustion
$\mathfrak{D}$ = gaseous diffusivity
$\mathfrak{D}_0$ = diffusion coefficient at reference conditions [see Eq. (11)]
E = activation energy
h = distance crystal protrudes above or is recessed below, the propellant surface
k = rate constant, $A\exp(-E/RT)$
m = mass flux associated with propellant components
m_T = total mass flux of propellant
n = burning rate pressure exponent, $d\ \ln r/d\ \ln P$
P = pressure
Q = heat release associated with combustion steps
Q_{fuel} = heat of pyrolysis of the fuel binder
Q_L = heat of gasification of the oxidizer
r = linear burning rate
R = gas constant
S = surface area
S_0 = total surface area
t_{ign} = ignition delay time
T = temperature
T_f = adiabatic flame temperature of the propellant
T_0 = initial temperature of the propellant
v = gas velocity
x^* = flame standoff distance
$\bar{x}^*$ = effective heat transfer distance, i.e., x^*/A_{fh}
W = molecular weight
α = weight fraction oxidizer
β_F = fraction of reactants involved in the primary diffusion flame
δ = reaction order
ζ = volume fraction of oxidizer in propellant
λ = thermal conductivity
η' = stoichiometric related coefficient [see Eq. (13)]
ξ^* = nondimensional standoff distance, $c_p m x^*/\lambda$
ρ = density
τ = characteristic time
ϕ_1 = first root of the first-order Bessel function (i.e., 3.83)

Subscripts

f = fuel binder
ox = oxidizer
FF = final flame conditions
s = the propellant surface conditions
AP = AP flame conditions
p = solid propellant
g = gas
PF = primary flame
D = diffusion
PD = primary diffusional distance

Introduction

A COMPOSITE solid propellant is a mixture of crystalline oxidizer and polymetric fuel binder, metal particles added as fuel, burning rate modifiers, processing aids, and curatives. The combustion of such a heterogeneous mixture is understandably complex, particularly when it is realized that the solid components are usually blended in three or four discrete sizes to aid in processing. In developing an analytical model for composite propellant combustion, these complexities are further compounded by an incomplete understanding of the various possible reactions present in composite propellants and the need for mathematical tractability in representing these reactions as well as those that are more fully understood. It follows, therefore, that it is unlikely that any one model can provide quantitative a priori burning rates of composite propellants.

Several models have been proposed in the past to describe the combustion of composite propellants.[1–6] In general, these models have been somewhat successful in correlating experimental data after the fact, but are not sufficiently accurate

Received September 24, 1969; revision received June 29, 1970. This work was sponsored by the Air Force Rocket Propulsion Laboratory under Contract AF-04611-67-C-0089 and Lockheed Propulsion Company. The Air Force technical monitor was Capt. C. E. Payne. The authors are indebted to D. E. Taylor and N. S. Cohen of Lockheed Propulsion Company for many stimulating discussions.

* Technical Specialist, Engineering Research Department. Associate Fellow AIAA.
† Technical Specialist, Engineering Research Department. Member AIAA.
‡ Senior Technical Specialist, Engineering Research Dept.

or complete to predict burning rate behavior a priori. Only the work by Hermance[4,5] considers the combustion problem on a sufficiently broad scale to be free of empirically derived constants. In that work however, an unrealistic description of the propellant surface was assumed. A heterogeneous reaction was assumed to occur in a cusp between the oxidizer crystals and the binder, the cusp resulting from the spherical regression of the oxidizer particles. Recent studies of extinguished propellant surfaces[7,8] have shown these assumptions to be invalid.

The objective of the present study was to develop a new analytical model of composite propellant combustion based on a realistic physical model, utilizing information derived both from recent experimental studies concerning the surface structure of extinguished propellants and previous analytical model efforts. The goal was not to predict burning rates a priori. Instead, the more realistic objective of predicting changes in burning rates for a given change in propellant formulation was considered. In keeping with the need for mathematical tractability, a propellant containing a unimodal oxidizer with binder was considered a simple, reasonable starting point. Through this approach, it is believed that a better understanding of the controlling factors in the combustion of a simple composite propellant can be derived.

A Physical Description of the Combustion Model

As a composite propellant burns, both the oxidizer and the binder are preheated by conduction as the surface proceeds into the propellant. At the propellant surface the initial decomposition step of both the binder and the oxidizer is endothermic. However, while still adsorbed on the surface, either set of products could possibly undergo further condensed phase reaction, resulting in a less endothermic and possibly an exothermic process at the surface. These products then pass into the gas phase, mix, and react. The characteristic time for gas phase reactions decreases with increasing pressure. Therefore, at low pressures (particularly with small AP particle sizes), one can expect the gases from both the oxidizer and the binder to mix completely before reacting. However, for increasing pressure or AP particle size, the reaction time becomes short and the mixing step may ultimately become the limiting process.

The idea of the propellant burning with a premixed flame at low pressures and as a diffusion flame at higher pressures has been proposed by Summerfield in his original granular diffusion flame model.[1] However, the premixed flame that was considered there, was formed by the fuel products and the decomposition product of the AP monopropellant flame. Hermance[5] also considered a similar flame structure (i.e., a premixed flame structure at low pressures and a diffusion controlled flame at high pressure). The difference with the flame structure proposed here is that the AP monopropellant flame is not considered as occurring at the propellant surface, but is considered as extending from the surface.

The nature of the burning surface at a variety of conditions has been studied extensively[7,8] by examining extinguished samples both with a visual microscope and a SEM.§ These studies (as well as others) have indicated that the AP crystals protrude from the burning surface (dome shaped) at low pressure and are recessed at high pressure. The sketch in Fig. 1 is typical of AP crystals at low pressures. No evidence has been observed for the cusp which formed the basis of the Hermance model.[4,5] However, the statistical approach of Hermance[4] is a significant contribution to modeling efforts of composite propellants and is employed in the present model (i.e., the model is based on the statistically average oxidizer particle).

The geometric relationship of the flame structure as proposed here is also sketched in Fig. 1. At low pressures (i.e., ambient to ~100 psi) the propellant is considered to burn as a premixed flame with the oxidizer and binder decomposition products mixing completely before reaction occurs. With increasing pressure, it becomes more difficult for the fuel products to diffuse into the stream above the oxidizer (and vice versa) and thus two reaction paths (i.e., oxidizing products + ammonia from the AP decomposition, vs binder products + AP-oxidizing products) become competitive. At higher pressures where reactions occur more rapidly, the oxidizing products react preferentially with the ammonia to yield the normal AP monopropellant flame before the binder products can diffuse into the oxidizer steam and react. Near the binder-oxidizer interface, it is presumed that some fraction of the oxidizing products react with the binder products at all pressures. However, the effect of these reactions becomes less important with increasing pressure.

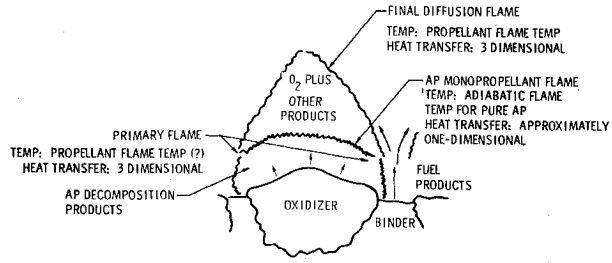

Fig. 1 The postulated flame structure for an AP composite propellant showing the primary flame and the AP monopropellant flame followed by the final diffusion flame.

The flame structure can be described by considering the two proposed reaction paths (see Fig. 1) A) $NH_3 + HClO_4$ products $\xrightarrow{\text{AP flame}}$ inert products + oxidizing species or B) fuel pyrolysis products (CH_2, CH_4, C, etc.) + $HClO_4$ products $\xrightarrow{\text{primary diffusion flame}}$ combustion products.

Whenever the AP flame occurs, it is followed by a diffusion flame (the 2-stage flame) where the oxygen-rich products of the flame (approx. 30% O_2) react with the fuel-rich binder pyrolysis products. This reaction should be dependent on mixing only, as the oxygen is heated to the temperature of the AP flame, 1400°K, and at this temperature would be expected to be very reactive. All the characteristics of a typical diffusion flame can be expected for this flame. It provides considerable energy to the surface at low pressures but has diminishing effect with increasing pressure.

In summary, three flames are considered in the model. The primary flame which is dependent on mixing and on kinetics (path B). The AP flame which is independent of mixing but kinetics-dependent (path A). The final flame which is strictly a diffusion flame (follows path A).

Modeling the microscopic flame structure of the statistically average oxidizer particle introduces a detailed, physical reality into the combustion model that has not been attempted previously. In the following section the details of the equations describing these flames are presented along with a discussion of the results and applications of the model.

Basic Equations of the Combustion Model

If one is to describe the physical nature of the burning surface for a random distribution of oxidizer in a fuel matrix, the surface can be assumed one dimensional and uniform, or a statistical description of the surface can be made. Both theoretical and experimental work[9,10] indicate that the size of the flame structure is of the same order as the oxidizer particle size, which tends to detract from the assumption of uniformity. Thus, the latter assumption seems preferable for completeness and physical reality. The statistical approach was first used by Hermance[4] who calculated the average intersection diameter for a plane passing through a randomly

§ SEM—Scanning electron microscope.

packed bed of spheres (i.e., the oxidizer particles) as being $(\frac{2}{3})^{1/2}D_0$ (see also Ref. 11). This value is then taken as the diameter of the statistically average oxidizer particle at the burning surface.

Conservation of Mass

For burning propellant the equation of mass continuity can be written as

$$m_T = r\rho_P = m_f(S_f/S_0) + m_{ox}(S_{ox}/S_0) \quad (1)$$

The first term on the right represents the total mass flow emanating from the fuel surface (including possible interface reactions) and the second corresponds to the oxidizer surface. This equation can be simplified further by requiring that the relative ratio of oxidizer to binder be maintained over a relatively long period of time (i.e., the ratio of oxidizer consumption to fuel consumption is equal to the weight ratio of oxidizer to fuel in the propellant).

Thus, averaged over the entire propellant surface the mass flux is

$$m_T = (m_{ox}/\alpha)(S_{ox}/S_0) = [m_f/(1-\alpha)](S_f/S_0) \quad (2)$$

It can be seen from Eq. (2) that the burning rate can be calculated from either of the two expressions. The first term of Eq. (2) implies that the burning rate of the propellant is determined on a macroscopic scale by the regression of the oxidizer. Utilization of the last term would imply that the binder regression is controlling. It is assumed here, that the regression of the oxidizer is the dominant characteristic of the combustion of composite propellants and therefore the first equality is used throughout the model.

Propellant Surface Geometry

To evaluate the area ratio in Eq. (2) the geometrical relationship between the oxidizer and the binder must be established. The area of the oxidizer that is exposed to reaction can be calculated by assuming that the portion of the crystal that protrudes above or is recessed below the surface is spherical, but always joining the fuel at the planar fuel surface. Thus,

$$\frac{S_{ox}}{S_o} = \frac{\zeta[6(h/D_0)^2 + 1]}{[6\zeta(h/D_0)^2 + 1]} \quad (3)$$

where ζ is the volume fraction of oxidizer in the propellant. The geometric factor h/D_0 represents the fractional distance the oxidizer protrudes above or is recessed below the surface and can be written

$$\frac{h}{D_0} = \frac{1}{2}\left(1 \pm \frac{1}{(3)^{1/2}}\right)\left(1 - \frac{r_{ox}}{r_f}\right) + r_{ox}\frac{t_{ign}}{D_0} \quad (4)$$

The second term in Eq. (4) is related to the ignition delay time as derived by Shannon[12] and utilized by Hermance.[4] Equations (3) and (4) permit the calculation of the oxidizer surface area ratio for eventual use in Eq. (2).

Conservation of Energy

In order to calculate the burning rate of a propellant using Eq. (2), the mass burning rate of the oxidizer must be evaluated. This is done assuming that global kinetics adequately describe the decomposition of the oxidizer. Utilizing an Arrhenius expression, the mass burning rate can be expressed as

$$m_{ox} = A_{ox}\exp(-E_{ox}/RT_s) \quad (5)$$

From Eq. (5) it can be seen that the surface temperature becomes a very critical factor in determining both the burning rate magnitude and pressure dependence.

Theories have been based on the assumption that the binder and the oxidizer are at different temperatures,[2] however, information describing such a distribution is not available. In the present model, an over-all averaged temperature is calculated, considering the energy of decomposition of both the binder and the oxidizer at the surface as well as the energy feedback from the flames to the surface by conduction. Thus, energy to raise propellant to T_s = (−) energy to vaporize oxidizer + (−) energy to vaporize fuel binder + energy arriving at surface from the various flames

$$m_T c_p(T_s - T_0) = -m_{ox}\frac{S_{ox}}{S_0}Q_L - m_f\frac{S_f Q_{fuel}}{S_0} + \beta_F Q_{PF} m_T \exp(-\xi_{PF}^*) + (1-\beta_F)m_{ox} \times \frac{S_{ox}}{S_0}[Q_{AP}\exp(-\xi_{AP}^*) + Q_{FF}\exp(-\xi_{FF}^*)] \quad (6)$$

where β_F is the fraction of the oxidizing reactants that react in the primary diffusion flame. Terms involving the exponentials represent the heat transferred from the various flame fronts to the propellant surface. The multiplying factor represents heat flux generated by the respective flame front, and the exponential function describes the fraction of generated heat conducted to the surface. By employing Eq. (2), the averaged surface temperature becomes

$$T_s = T_0 - \alpha\frac{Q_L}{c_p} - (1-\alpha)\frac{Q_{fuel}}{c_p} + (1-\beta_F)\alpha \times \left[\frac{Q_{AP}}{c_p}\exp(-\xi_{AP}^*) + \frac{Q_{FF}}{c_p}\exp(-\xi_{FF}^*)\right] + \beta_F\frac{Q_{PF}}{c_p}\exp(-\xi_{PF}^*) \quad (7)$$

The evaluation of the nondimensional standoff distances, β_F and the energy terms is discussed in the following sections.

Gas Phase Phenomena

The standoff distance for a kinetically limited one-dimensional flame can be written as[4]

$$x^* = m/kP^\delta = m/P^\delta A\exp(-E/RT) \quad (8)$$

where k now represents a pseudo rate constant (i.e., the Arrhenius rate constant combined with various proportionality constants), and δ is an arbitrary reaction order. Combining Eq. (8) with the definition of the nondimensional flame standoff and solving for the mass burning rate yields

$$m = P^{\delta/2}(k\lambda\xi^*/c_p)^{1/2} \quad (9)$$

which is the same form that results from more rigorous derivations.[13,14] The principal difference between Eq. (9) and the more rigorous equations involves the relationship between ξ^* and the conservation equations. In the present derivations ξ is simply related to the thermal conduction whereas the more rigorous derivations involve a more complete description of the reactions taking place and the flow interaction between the products and reactants. The more rigorous derivations would be unjustified in the present application because of the lack of precise knowledge concerning the reactions.

Diffusional Mixing

Diffusional processes are important in the model becasue of the physical separation of the binder and oxidizer. As reaction times become short with increasing pressure, the diffusional processes should become significant and perhaps even dominant. The diffusional mixing distance is the variable that causes this in the model, and will be discussed here. The characteristic diffusional time can be written dimensionally as

$$\tau_D \propto d^2/\mathfrak{D} \quad (10a)$$

or

$$\tau_D \propto d/v \quad (10b)$$

Equation (10b) applies to very short flames where the mixing time is the transport time. Equation (10a) is the more conventional characteristic time usually associated with diffusional processes. The gaseous diffusivity is[15]

$$\mathfrak{D} = \mathfrak{D}_0 T^{1.75}/P \tag{11}$$

and the diffusional standoff distance becomes ($x^* = v\tau$)

$$x_D^* \propto (m/\rho_g) d^2 P/\mathfrak{D}_0 T^{1.75} \tag{12a}$$

or

$$x_D^* \propto d \tag{12b}$$

[Equation (12a) is essentially the form used by Hermance.[5]]

From Eq. (12) and the ideal gas law ($\rho_g \propto P$) it is apparent that there is no pressure dependence for a flame that is simply a diffusion flame. This is the conclusion reached by Nachbar[3] in his attempts to model composite propellant combustion based on diffusional limitations. Because of the fact that the burning rate of composite propellants does vary with pressure, Nachbar concluded that the propellant flame is not a simple diffusion flame. This corroborates one of the basic assumptions of the present model (i.e., "the flame" is a combination of several complicated flames). However, under certain conditions, and for limited pressure regimes, some composite propellants exhibit a plateau in the burning rate curve where the burning rate does not vary with pressure [for example see propellant A-35 reported in Ref. (16)]. This indicates that under certain restricted conditions, the combustion of composite propellants can be diffusion-limited.

A successful detailed analysis for tall diffusion flames was reported by Burke and Schumann in 1928.[17] Because of the circular symmetry involved in their analysis, it appears to be very appropriate for the present problem of a spherical oxidizer crystal surrounded by a fuel. A complete review of the analysis and assumptions has been made by Williams.[18] A modified solution to the original Burke-Schumann analysis that is not limited to tall flames (as suggested by Williams) is summarized by the equation for the diffusional mixing length

$$x_D^* = 2c_2\eta^1/m\{1 + (2c_2\phi'/mb)^2]^{1/2} - 1\} \tag{13}$$

where c_2 is related to the surface temperature and the diffusion coefficient of Eq. (11). The term η' is related to the mixture ratio of the flame and the surface geometry. ϕ_1 is a constant, and b is the distance from the center of a crystal to the center of the adjacent binder. This characteristic dimension of the surface can be shown to be

$$b = (D_0/2)\{[\pi/6][1 + \rho_{ox}(1 - \alpha)/\rho_f\alpha]\}^{1/3} \tag{14}$$

When the product mb is sufficiently small (e.g., low burn rate or small particles), Eq. (13) reduces to the form of Eq. (12b). For high burning rates and/or large particle sizes, mb becomes large and Eq. (13) approaches the tall flame limit represented by Eq. (12a). A comparison of the results based on both the tall and the short flame analyses is made in a later section.

Flame Standoff Distances

From the aforementioned equations the calculated flame height represents the maximum height of the flame above the center of the oxidizer crystal. The actual flame shape will be symmetrical around the center line of the crystal but will vary with radial distances forming a somewhat conical configuration above the oxidizer (see Fig. 1). For the present application an average, effective flame height has been defined assuming that some fraction of the calculated flame height corresponds to the distance a one-dimensional flame would be from the surface in order to deliver the same amount of energy to the surface as the actual flame. Thus, the effective heat transfer distance becomes

$$\bar{x}_D^* = A_{fh} x_D^* \tag{15}$$

where A_{fh} is the average flame height factor and has a value between zero and one.

Equation (15) is used directly to calculate the final diffusion flame standoff distance. The distance calculated in this manner is the distance between the AP flame and the effective diffusion flame heat release point. In order to incorporate these results into the surface temperature calculation, the diffusional length must be added to the AP flame standoff to give the total distance from the surface that the heat release takes place. In nondimensional form this is

$$\xi_{FF}^* = c_p m_{ox}(x_{AP}^* + \bar{x}_D^*)/\lambda \tag{16}$$

Similarly, the primary flame standoff distance is the sum of two terms. In the primary flame the components must mix together and then react, so that there is a diffusion distance followed by the distance that it takes the ingredients to react. Again in the nondimensional form

$$\xi_{PF}^* = c_p m_T(\bar{x}_{PD}^* + x_{PF}^*)/\lambda \tag{17}$$

$\bar{x}_{PD}^*$ is calculated from Eq. (13) where the temperature is the propellant surface temperature and x_{PF}^* is calculated from Eq. (8). The third nondimensional standoff distance that is needed to evaluate Eq. (7) is that of the oxidizer flame. This is simply

$$\xi_{AP}^* = (c_p m_{ox}/\lambda)x_{AP}^* = c_p m_{ox}^2/\lambda k_{AP} P^\delta \tag{18}$$

Competing Flame

From the general discussion of the model and the primary flame it is apparent that there is a range of pressures where the monopropellant flame and the primary flame are competing for the reactive oxidizer species. Mathematically this is accounted for by the term β_F in Eq. (7), where β_F is the fraction of the oxidizing reactants that react in the primary flame. At low pressures β_F is unity. In other words, the combined primary flame mixing and reacting distances are less than the AP flame height, and therefore all of the oxidizing species react directly with the binder products rather than with the ammonia-derived fuel species from the AP. As pressure and burning rate increase, the AP flame height is reduced considerably [see Eq. (18)], the primary flame reactive distance is reduced, but the primary diffusive distance is increased or held constant [see Eq. (12)]. Thus near the center of the crystal where the diffusive distance is greatest, the oxidizing species react preferentially with the ammonia derivatives in the AP flame, and β_F is between zero and one. At high pressure, the AP flame standoff becomes very small as does the primary flame reacting distance, while the diffusive distances are relatively large. Under these conditions a very small amount of the original oxidizing species reacts with the binder products in the primary flame near the binder-oxidizer interface, and β_F approaches zero.

The numerical evaluation of β_F is made, by assuming the diffusional flame shape to be either parabolic or conical above the oxidizer particle (calculations have been made for both cases). The intersection of the AP and primary flames can be projected onto the surface of the oxidizer crystal and the area corresponding to each flame determined. Numerically, then, β_F becomes the fraction of AP surface whose products enter into the primary flame. The results are slightly different depending on the assumed flame shape. For a parabolic shape the transition from $\beta_F = 1$ to $\beta_F \sim 0.1$ (β_F is always greater than zero) occurs over a more narrow pressure range than if a conical flame is assumed. The parabolic flame shape was utilized in the calculations discussed below.

Ingredient Decomposition

The dissociative sublimation of ammonium perchlorate gives ammonia and perchloric acid and the reaction is endothermic by 56 kcal/mole or approximately 480 cal/g. However, recent work[19-23] seems to indicate that this is not the only reaction occurring at the AP surface during deflagration.

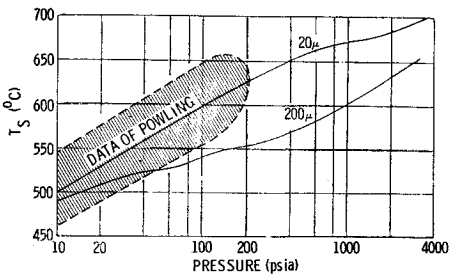

Fig. 2 Variation of surface temperature with pressure calculated for two AP/polysulfide propellants and compared to the data of Powling.[28]

It appears likely that there are reactions (other than just the simple sublimation) occurring in the thin molten layer that has been observed on the surface of the deflagrating AP single crystals[21,22] and in composite propellants.[7] Exothermic reactions occurring in the thin layer on the AP surface will result in a less endothermic value of the term Q_L than the 480 cal/g quoted above, perhaps even to the extent of being exothermic. Because these reactions take place in a very thin zone near the surface, the entire process can be ascribed to the surface without considering the complications that arise from equations describing reactions below the AP surface.

The stoichiometry of the reactions enters into Eq. (15) in the term η'. In evaluating this term, the stoichiometric ratio of oxidizer to fuel was calculated assuming CO_2, H_2O, SO_2, etc., as final products. The calculated ratios for a polysulfide binder (PS), a polyurethane binder (PU), and a polybutadiene binder (PBAA) with AP as the oxidizer are 4.9, 6.2, and 9.0, respectively.

The pyrolysis of the binder enters into the equations of the model in determining the surface geometry, the surface temperature and the gaseous fuel species. The energy required to break up the binder has a principal effect in the equation used to calculate the surface temperature. It can be seen that the effect of a larger value of Q_{fuel} (more endothermic) has a cooling effect on the surface temperature and thus [through Eq. (2) and (5)] reduces the burning rate. Although Q_{fuel} is not precisely known, a value on the order of 0–200 cal/g seems reasonable for a typical hydrocarbon binder (Hermance[4,5] used 175 cal/g). For more energetic binders Q_{fuel} would decrease while for a very stable binder, such as fluorocarbon, Q_{fuel} would be considerably larger (more energy is required to break up the polymer).

The effect of the binder pyrolysis is accounted for on a microscopic scale in Eq. (4) where the geometric relationship between the oxidizer and binder is established. A linear regression rate for the binder is calculated from the same form of equation as that of the oxidizer:

$$m_f = A_f \exp(-E_f/RT_s) \tag{19}$$

Because the regression of the oxidizer is taken as the rate controlling step in the combustion, Eq. (19) has only a secondary effect on the burning rate of the propellant, influencing the value of S_{ox} through Eqs. (3) and (4).

Gas Phase Heat Releases

In Eq. (7) there is a gas phase heat release associated with each of the three flames. These energy releases are determined from an over-all energy balance assuming that equilibrium is attained in the flames, and that the system, is adiabatic. The heat release associated with the monopropellant flame is

$$Q_{\text{AP}} = c_p(T_{\text{AP}} - T_0) + Q_L \tag{20}$$

For an averaged specific heat of 0.3 cal/g°C the sensible energy term represents 330 cal/g ($T_{\text{AP}} \sim 1400$°K). Therefore, adding this to the value of 480 cal/g that is associated with the dissociative sublimation of AP, 810 cal/g are needed to achieve the adiabatic flame temperature. This represents the maximum value that Q_{AP} can have. However, if half of the available energy is released in the liquid surface layer, then Q_{AP} would be 405 cal/g and Q_L will be on the order of 75 cal/g, etc.

The final flame heat release is calculated from an over-all energy balance considering the entire propellant composition, and can be written as

$$Q_{FF} = (c_p/\alpha)\{(T_s - T_0) - \alpha(T_{\text{AP}} - T_0) + [(1 - \alpha)/c_p]Q_{\text{fuel}}\} \tag{21}$$

The heat release associated with the primary flame is

$$Q_{PF} = c_p(T_f - T_0) + \alpha Q_L + (1 - \alpha)Q_{\text{fuel}} \tag{22}$$

where Q_{PF} is based on the mass flux of the propellant rather than that of the oxidizer as was Q_{FF}. In making calculations the same adiabatic flame temperature was used in both Eqs. (21) and (22), assuming that the final reaction products are the same in both the primary flame and the final flame. Because of the lack of precise information concerning the reactants, the intermediate products, and final products, this appears to be a reasonable assumption.

Results

In the preceding equations, the burning rate appears in a transcendental form requiring an iterative solution. The principal equations involved are Eqs. (2, 3, 5, and 7) with the various terms defined appropriately. The equations were solved numerically on an IBM-360 Model 40 digital computer, iterating on the surface temperature, at a given pressure. After reaching a solution the pressure was incremented and a new iteration begun.

Experimental data reported by Bastress[24] for a series of unimodal polysulfide propellants have been used for comparative purposes. These data represent the most complete set of burning rate data available for a series of propellants covering a very wide range of pressures including various concentrations and unimodal particle size distributions.

Parameter Values

Part of the philosophy behind the development of the model was to describe the combustion process in as realistic a manner as possible and then to relate the effects of various combustion trends to individual ingredients and/or combustion mechanisms. To accomplish this, values of the various parameters must be determined. This becomes a difficult and yet a critical part of the model evaluation because the majority of the parameter values are either unknown or known to an approximate extent. However, this problem can be alleviated somewhat by determining relative effects of the parameters and using relative values for those that have a small effect on the over-all results. A second approach is to evaluate the calculations in terms of as many known experimental facts as is possible. In this manner the possible deleterious effects caused by unknown parameter values can be reduced.

For example, variations in the value of S_{ox}/S_0 were determined to have a very minor effect on the calculated burning rate curve. Varying t_{ign} in Eq. (4) over a very large range of values had a significant effect on the calculated values of h/D_0, a lesser effect on the value of S_{ox}/S_0 and virtually no effect on the burning rate. Thus, the parameters involved only in Eq. (4), (i.e., A_f, E_f, and t_{ign}), have such a small influence on the burning rate that the particular value used for these parameters is not important. E_f was taken as 15 kcal/mole,[25,26] and A_f and r_{ign} were adjusted to give consistent values of h/D_0. Experimental studies[7,8,24] indicate that h/D_0 should be positive at low pressures, zero somewhere in the range of 300 to 600 psi. and negative at higher pressures. All of the calculations discussed below are consistent with these observations.

Variations in the gas phase physical properties, λ, c_p, $\mathfrak{D}_0$ and A_{fh} were observed to have a significant effect on the magnitude of the burning rate. However, values of these parameters will not be dependent on propellant formulation. By assigning a reasonable, constant value to each of these parameters, calculations for various propellant formulations become relative. An a priori prediction of absolute values of the burning rate is excluded, but calculated trends will still be valid. The averaged values of these four parameters are listed in Table 1, along with other parameter values used in the calculations.

The adiabatic flame temperatures for the given propellant and for AP burning as a monopropellant are calculated from thermochemistry as is the molecular weight of the combustion gases. The kinetic constants for the AP combustion, k_{AP} and δ_{AP}, are both calculated from the known burning rate of AP at 70 atm. The gas phase activation energy was taken as 30 kcal/mole.[27]

Surface Temperature and Flame Standoff Distances

The surface temperature has a very significant effect on the calculated burning rate, and therefore, is very important within the model. Values for the surface temperature can be obtained from the work of Powling[28] who measured the surface temperature of several propellant systems at low pressures using an infrared technique. Surface temperatures determined in the calculations discussed below for propellants containing 20 μ and 200 μ oxidizer (α = 0.70) are compared to Powling's work in Fig. 2. The agreement is very reasonable. From Eq. (5) the effect of the surface temperature on the burning rate is influenced greatest by the parameters A_{ox} and E_{ox}. A change in either of these parameters causes a significant change in the calculated surface temperature, and a corresponding (but reduced) change in the burning rate magnitude. However, if A_{ox} and E_{ox} are varied in such a way that the surface temperature at a given pressure is approximately constant, then the burning rate magnitude is changed only slightly over the pressure range. A value of 22 kcal/mole was used as being representative.[28,29] of the activation energy for the combustion of AP. A_{ox} was adjusted to give reasonable agreement with Powling's data.

The flame standoff distances also have a very important effect on the surface temperature and subsequently on the burning rate. The magnitude of the flame standoff distance is not well-known[9,10]; the consensus of opinion indicating only that there are energy releases between the surface and 1000 μ above it. Within the framework of the physical model, there is no one flame standoff distance but there is an entire spectrum of energy releases above the propellant surface, because of the three different flames and the nature of their shape. The heat transfer distance as calculated by the model varied from values of ~300 μ at one atm for the 200 μ propellant to ~5 μ for the AP flame of the 20 μ propellant above 2000 psi (followed by a 20 μ tall final diffusion flame). The trend was for decreasing flame height with increasing pressure and with decreasing particle size. Thus, the model agrees with experimental observations that there are a variety of energy releases between the propellant surface and distances less than 1000 μ above the surface.

Evaluating the various parameters as described previously, leaves the following parameters unevaluated, δ, Q_L, Q_{fuel}, and k_{PF}. Approximate values for the first two have been discussed previously, and the reaction rate order is expected to have a value between one and two for a gas phase reaction (a value nearer two appears most likely). A recent study has reported the activation energy of the ClO_2—CH_4 reaction (i.e., the primary flame) as 15 kcal/mole.[28] However the prefactor is not defined. Parametric calculations were made with the model comparing the results with the known characteristics of AP composite propellants to arrive at reasonable values of these parameters.

Table 1 "Standard" parameter values

Propellant Data	**Flame Parameters**
α = 0.70	δ_{PF} = 1.5
T_f = 2545°K	k_{PF} = 30 g/(cm³-sec-atm$^\delta$)
T_0 = 27°C	$\mathfrak{D}$ = 0.16 cm²/sec (at room temperature and pressure)
W = 26.2 g/mole	λ = 0.0003 cal/cm-sec-°K
D_0 = 20 μ	c_p = 0.3 cal/g-°K
ρ_f = 1.27 g/cc	A_{fh} = 0.3
ρ_{ox} = 1.95 g/cc	E_{PF} = 15 kcal/mole
Binder Data	**Ammonium Perchlorate Data**
E_f = 15 Kcal/mole	T_{AP} = 1400°K
A_f = 2.5 × 10³ g/cm²-sec	δ_{AP} = 1.8
Q_{fuel} = 50 cal/g (endothermic)	E_{ox} = 22 Kcal/mole
	A_{ox} = 3 × 10⁵ g/cm²-sec
Internally Calculated Parameters	Q_L = −120 kcal/g
	E_{AP} = 30 Kcal/mole
k_{AP} = 1.12 g/(cm³-sec-atm$^\delta$)	
Q_{PF} = 605 cal/g	
Q_{PF} = 654 cal/g	

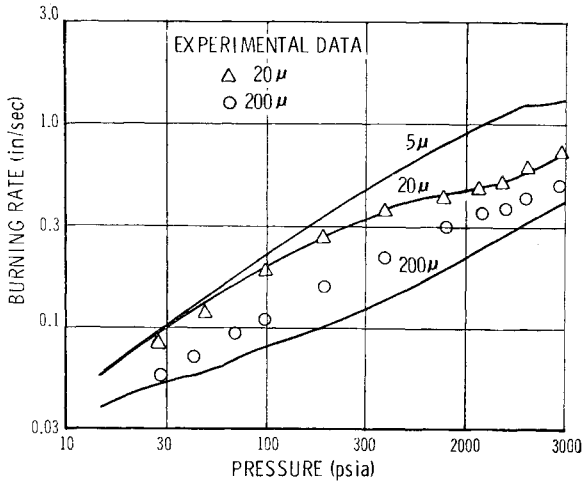

Fig. 3 The calculated burning rates for three 70% AP/-polysulphide propellants varying the AP particle size.

Effect of Particle Size, Concentration, and Initial Temperature

From the basic considerations of the model and the form of the equations, it can be seen that the surface temperature will be less for lower oxidizer concentrations which will reduce the burning rate. On the other hand, the diffusional distances will decrease with decreasing particle size increasing the burning rate. Both of these trends are qualitatively consistent with experimental observation. The effect of particle size is seen in Fig. 3 where the results are plotted for calculations of 5, 20, and 200 μ particle sizes. The available experimental data for the 20 and 200 μ propellants[24] are included. The predicted change in the burning rate due to the particle size is somewhat greater than that observed experimentally. Within the model, the particle size enters the calculations in the equations for the diffusional lengths and in calculating the oxidizer surface area. The latter is a secondary effect compared to the former, indicating that the discrepancy is probably in the form of the equations describing the diffusional distances. In Fig. 3, Eqs. (10b) and (12b) were employed with the diffusional distance corresponding to the oxidizer particle size. Utilization of Eqs. (10a) and (12a) resulted in a much greater discrepancy between the calculations and the data. Therefore, Eqs. (10b) and (12b) corresponding to a short diffusional distance have been used throughout the calculations.

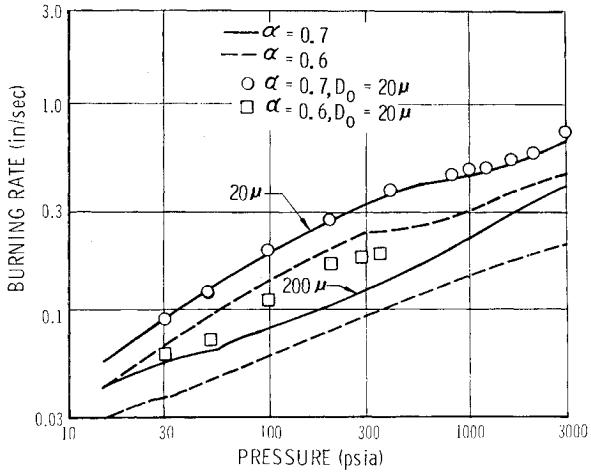

Fig. 4 The calculated effect of oxidizer concentration on burning rate for 20 and 200μ AP/polysulphide propellants.

In terms of the model, the primary flame is controlling (i.e., $\beta_F = 1.0$), up to the break point in the curves shown in Fig. 3. This transition occurs at ~50, at ~800 and at ~2000 psi for the 200, 20, and 5 μ propellant, respectively. The flatter portion of the curves indicate that the diffusional aspects of the primary flame are dominating the calculation in those regions. Increasing the pressure beyond this point causes the curve to break upward again as the AP flame begins to have a greater influence on the burning rate (i.e., $\beta_F < 1.0$).

The numerical calculations for varying the concentration from 60 to 70% oxidizer in a polysulfide binder with both 20 and 200 μ AP are displayed in Fig. 4. The calculations are close to observed trends over the entire pressure range. From experimental data,[24] the dependence of burning rate on concentration is on the order of 5.0 (i.e., $(1/r)(dr/d\alpha)$). The calculated dependence is 4.

An important characteristic of propellant combustion that can be used in evaluating the model is the temperature sensitivity (denoted as $d \ln r/dT_0$). Typical values for bimodal composite propellants are on the order of 0.11–0.13%/°F (measured at 1000 psi). The values calculated at 1000 psi are 0.29 and 0.11%/°F for the 200 μ and 20 μ propellants, respectively. The calculations indicate that the temperature sensitivity increases with increasing pressure as well as with increasing particle size. Both of these trends are consistent with recent experimental studies relating to propellant temperature sensitivities.[30] The calculations also indicated an increased sensitivity with increased oxidizer content.

Of the various parameter values required by the model to give the foregoing agreement with experimental data that has been achieved, the most significant is probably the value of Q_L, the heat release of the oxidizer at the burning surface. It was found that a value on the order of −100 to −200 cal/g was required to meet the several requirements stipulated above. For example, if a value of 0 to −100 were used for Q_L, the temperature sensitivity would be reduced by at least a factor of two, the concentration dependence would be reduced to almost zero, and the particle size dependence would be increased even above that of Fig. 3. Recalling the previous discussion of Q_L, these results indicate that on the order of 75% of the energy available during the combustion of AP is released at the burning surface, apparently in the liquid layer. Therefore, any modification of the AP that might affect the liquid layer could have profound effects on the burning rate of composite propellants.

Conclusions

The calculated results of the proposed model have not only been compared with burning rate data, but also with the particle size dependence and concentration dependence of burning rates, with temperature sensitivity data, as well as with the variation of surface temperature and pressure exponent with pressure. In addition, the flame structure and surface geometry have also been considered. This has permitted the evaluation of the results in terms of a very broad scope of combustion, rather than simply considering the observed burning rate as a function of pressure as is sometimes done.

The results indicate that the model is capable of describing the various qualitative combustion characteristics observed in composite propellants (i.e., high slope at low pressure, reduced slope and possible plateau burning at intermediate pressures, and increased slope at high pressures). The calculations indicate that the predicted dependence of burning rate on oxidizer concentration is essentially the same as observed experimentally. The calculated dependence of burning rate on oxidizer particle size is somewhat greater than observed experimentally. The dependence on initial temperature is in qualitative agreement with data showing a trend to increase with both pressure and particle size. The model calculates as output the mean propellant surface temperature, flame standoff distance, and a geometric factor describing oxidizer particle shape. Results show the calculated values to be in agreement with experimental programs studying the surface temperatures, flame structure, and surface structure of composite propellants.

References

[1] Summerfield, M. et al., "The Burning Mechanism of Ammonium Perchlorate Propellants," *ARS Progress in Astronautics and Rocketry Vol. I: Solid Propellant Rocket Research*, Academic Press, New York, 1960, pp. 141–182.

[2] Chaiken, R. F. and Anderson, W. H., "The Role of Binder in Composite Propellant Combustion," *ARS Progress in Astronautics and Rocketry, Vol. I: Solid Propellant Rocket Research*, Academic Press, New York, 1960, pp. 227–249.

[3] Nachbar, W., "A Theoretical Study of the Burning of a Solid Propellant Sandwich," *ARS Progress in Astronautics and Rocketry, Vol. I: Solid Propellants Rocket Research*, Academic Press, New York, 1960, pp. 207–226.

[4] Hermance, C. E., "A Model of Composite Propellant Combustion Including Surface Heterogeneity and Heat Generation," *AIAA Journal*, Vol. 4, No. 9, Sept. 1966, pp. 1629–1637.

[5] Hermance, C. E., "A Detailed Model of the Combustion of Composite Solid Propellants," *Proceedings of the ICRPG/AIAA 2nd Solid Propulsion Conference*, Anaheim, Calif., June 6–8, 1967, pp. 89–103.

[6] Fenn, J. B., "A Phalanx Flame Model for the Combustion of Composite Solid Propellants," *Combustion and Flame*, Vol. 12, No. 3, June 1968, pp. 201–216.

[7] Boggs, T. L., Derr, R. L., and Beckstead, M. W., "The Surface Structure of Ammonium Perchlorate Composite Propellants, *AIAA Journal*, Vol. 8, No. 2, Feb. 1970, pp. 370–372.

[8] Derr, R. L. and Boggs, T. L., "Role of Scanning Electron Microscopy in the Study of Solid Propellant Combustion: Part III. The Surface Structure and Profile Characteristics of Burning Composite Solid Propellants," *Combustion Science and Technology*, Vol. 2, No. 2, 1970, pp. 219–238.

[9] Derr, R. L. and Osborn, J. R., "Composite Propellant Combustion," *AIAA Journal*, Vol. 8, No. 8, Aug. 1970, pp. 1488–1491.

[10] Povinelli, L. A., "A Study of Composite Solid-Propellant Flame Structure Using a Spectral Radiation Shadowgraph Technique," *AIAA Journal*, Vol. 3, No. 9, Sept. 1965, pp. 1593–1598.

[11] Blum, E. H. and Wilhelm, R. H., "A Statistical Geometric Approach to Random-Packed Beds," *AIChE—Industrial Chemical Engineering Symposium Series No. 4* (London Inst. of Chemical Engineers), 1965, pp. 4:21–4:27.

[12] Shannon, L. H. and Petersen, E. E., "Deflagration Characteristics of Ammonium Perchlorate Strands," *AIAA Journal*, Vol. 2, No. 1, Jan. 1964, pp. 168–169; also Shannon, L. J., "Effects of Particle Size and Initial Temperature on the Deflagration of Ammonium Perchlorate," Ph.D. thesis, 1963, Univ. of California, Berkeley, Calif.

[13] Johnson, W. E. and Nachbar, W., "Deflagration Limits in the Steady Linear Burning of a Monopropellant with Application

to Ammonium Perchlorate," *Eighth Symposium (International) on Combustion*, Williams and Wilkins, Baltimore, Md., 1962, pp. 678–689.

[14] von Kármán, T., "The Present Status of the Theory of Laminar Flame Propagation," *Sixth Symposium (International) on Combustion*, Reinhold, New York, 1957, pp. 1–11.

[15] Penner, S. S., *Chemistry Problems in Jet Propulsion*, Pergamon Press, Los Angeles, 1957, p. 246.

[16] Beckstead, M. W. and Culick, F. E. C., "A Comparison of Analysis and Experiment for Solid Propellant Combustion Instability," to be published in *AIAA Journal*, 1971.

[17] Burke, S. P. and Schumann, T. E. W., "Diffusion Flames," *Industrial and Engineering Chemistry*, Vol. 20, 1928, p. 998; also *First and Second Symposium on Combustion*, The Combustion Institute, Pittsburgh, Pa., 1965, pp. 2–11.

[18] Williams, F. A., *Combustion Theory*, Addison-Wesley, 1965, pp. 37–45.

[19] Pellett, G. L. and Cofer, G. L., III, "High-Temperature Decomposition of Ammonium Perchlorate Using CO_2 Laser-Mass Spectrometry," AIAA Paper 69-143, New York, 1969.

[20] Pellett, G. L. and Saunders, A. R., "Heterogeneous Decomposition of Ammonium Perchlorate-Catalyst Mixtures Using Pulsed Laser Mass Spectrometry," AIAA Paper No. 68-149, New York, 1968.

[21] Hightower, J. D. and Price, E. W., "Combustion of Ammonium Perchlorate," *Eleventh Symposium (International) on Combustion*, The Combustion Institute, Pittsburgh, Pa., 1967, pp. 1373–1380.

[22] Beckstead, M. W. and Hightower, J. D., "Surface Temperature of Deflagrating Ammonium Perchlorate Crystals," *AIAA Journal*, Vol. 5, No. 10, Oct. 1967, pp. 1785–1790.

[23] Waesche, R. H. W. and Wenograd, S., "Calculation of Solid Propellant Burning Rates from Condensed-Phase Decomposition Kinetics," AIAA Paper No. 69-145, New York, 1969.

[24] Bastress, E. K., "Modification of the Burning Rates of Ammonium Perchlorate Solid Propellants by Particle Size Control," Ph.D. thesis, 1961, Princeton Univ., Princeton, N. J.

[25] Hansen, J. G. and McAlevy, R. F., III, "Energetics and Chemical Kinetics of Polystyrene Surface Degradation in Inert and Chemically Reactive Environments," *AIAA Journal*, Vol. 4, No. 5, May 1966, pp. 841–848.

[26] Anderson, W. H. et al., "A Model Describing Combustion of Solid Composite Propellants Containing Ammonium Nitrate," *Combustion and Flame*, Vol. 3, 1959, pp. 301–318.

[27] Combourieu, J., et al., "Ammonium Perchlorate Combustion Analogue: Ammonia-Chlorine Dioxide Flames," *AIAA Journal*, Vol. 8, No. 3, March 1970, pp. 594–597.

[28] Powling, J., "Experiments Relating to the Combustion of AP-Based Propellants," *11th International Combustion Symposium*, The Combustion Institute, Pittsburgh, Pa., 1967, pp. 447–456.

[29] Coates, R. L., "Linear Pyrolysis Rate Measurements of Propellant Constituents," *AIAA Journal*, Vol. 3, No. 7, July 1965, pp. 1257–1261.

[30] Cohen, N. S., unpublished data obtained on Contract F04611-69-C-0072, Feb. 1970, Lockheed Propulsion Co., Redlands, Calif.

DECEMBER 1970 AIAA JOURNAL VOL. 8, NO. 12

Calibration and Use of Electrostatic Probes for Hypersonic Wake Studies

I. P. FRENCH,* R. A. HAYAMI,† T. E. ARNOLD,* AND M. STEINBERG*
AC Electronics—Defense Research Laboratories, Santa Barbara, Calif.

AND

J. P. APPLETON‡ AND A. A. SONIN§
Massachusetts Institute of Technology, Cambridge, Mass.

An experimental shock-tube program was undertaken in order to calibrate spherical and cylindrical electrostatic probes that may be used to make point ion density measurements in continuum flowing plasmas. The empirically derived formula that relates ion density to measured probe current was obtained in terms of appropriate similarity parameters: the Nusselt number for mass transfer of positive ions, dimensionless probe potential, ratio of Debye length to probe radius, and flow Reynolds number. The empirical correlation was used to interpret ion currents collected by a radial array of negatively biased spherical probes, which were positioned so as to intercept the ionized wake of a hypervelocity model in a ballistics range. Integrated ion densities were found to be in good accord with integrated electron densities which were simultaneously measured using microwave methods.

1. Introduction

IT has long been recognized that our understanding of the structure and radar-scattering characteristics of the wakes of hypervelocity projectiles might be significantly advanced if time-resolved point measurements of electron density were available in the wakes. Although ballistics ranges do provide an appropriate laboratory environment for making such measurements, and indeed reliable measurements of average electron density as a function of distance behind the projectile have been obtained,[1,2] attempts at measuring local electron density with electrostatic probes have so far been hampered by difficulties with the interpretation of the probe signal.[3,4]

In a recent paper, Sutton[5] proposed a ballistics range experiment that might allow such measurements to be performed with cylindrical collision-free Langmuir probes, held in tension so as to avoid the problem of probe bending. To operate the probe in the collision-free regime, and at the same time have a turbulent wake, requires relatively large ballistics models and low environmental pressures. (Sutton's calculations were based on the theoretically computed wake conditions behind a 6.8 cm diam sphere traveling at 4.72 km sec^{-1} in an ambient pressure of 10 torr.) Unfortunately, the bal-

Received October 13, 1969; revision received March 30, 1970. This work was supported by ARPA and monitored by SAMSO, under Contract F04701-69-C-0125.

* Staff Scientist.
† Staff Engineer. Member AIAA.
‡ Associate Professor, Mechanical Engineering Department.
§ Associate Professor, Mechanical Engineering Department. Member AIAA.